

University of Groningen

Long-range order of Ni²⁺ and Mn⁴⁺ and ferromagnetism in multiferroic (Bi_{0.9}La_{0.1})₂NiMnO₆ thin films

Langenberg, E.; Rebled, J.; Estrade, S.; Daumont, C. J. M.; Ventura, J.; Coy, L. E.; Polo, M. C.; Garcia-Cuenca, M. V.; Ferrater, C.; Noheda, B.

Published in:
Journal of Applied Physics

DOI:
[10.1063/1.3524278](https://doi.org/10.1063/1.3524278)

IMPORTANT NOTE: You are advised to consult the publisher's version (publisher's PDF) if you wish to cite from it. Please check the document version below.

Document Version
Publisher's PDF, also known as Version of record

Publication date:
2010

[Link to publication in University of Groningen/UMCG research database](#)

Citation for published version (APA):

Langenberg, E., Rebled, J., Estrade, S., Daumont, C. J. M., Ventura, J., Coy, L. E., Polo, M. C., Garcia-Cuenca, M. V., Ferrater, C., Noheda, B., Peiro, F., Varela, M., & Fontcuberta, J. (2010). Long-range order of Ni²⁺ and Mn⁴⁺ and ferromagnetism in multiferroic (Bi_{0.9}La_{0.1})₂NiMnO₆ thin films. *Journal of Applied Physics*, 108(12), 123907-1-123907-4. [123907]. <https://doi.org/10.1063/1.3524278>

Copyright

Other than for strictly personal use, it is not permitted to download or to forward/distribute the text or part of it without the consent of the author(s) and/or copyright holder(s), unless the work is under an open content license (like Creative Commons).

The publication may also be distributed here under the terms of Article 25fa of the Dutch Copyright Act, indicated by the "Taverne" license. More information can be found on the University of Groningen website: <https://www.rug.nl/library/open-access/self-archiving-pure/taverne-amendment>.

Take-down policy

If you believe that this document breaches copyright please contact us providing details, and we will remove access to the work immediately and investigate your claim.

Downloaded from the University of Groningen/UMCG research database (Pure): <http://www.rug.nl/research/portal>. For technical reasons the number of authors shown on this cover page is limited to 10 maximum.

Long-range order of Ni^{2+} and Mn^{4+} and ferromagnetism in multiferroic $(\text{Bi}_{0.9}\text{La}_{0.1})_2\text{NiMnO}_6$ thin films

E. Langenberg,^{1,a)} J. Rebled,² S. Estradé,² C. J. M. Daumont,³ J. Ventura,¹ L. E. Coy,¹ M. C. Polo,¹ M. V. García-Cuenca,¹ C. Ferrater,¹ B. Noheda,³ F. Peiró,² M. Varela,¹ and J. Fontcuberta⁴

¹*Departament Física Aplicada i Òptica, Universitat de Barcelona, Martí i Franquès 1, 08028 Barcelona, Spain*

²*Departament Electrònica, Universitat de Barcelona, Martí i Franquès 1, 08028 Barcelona, Spain*

³*Zernike Institute for Advanced Materials, University of Groningen, Groningen 9747AG, The Netherlands*

⁴*Institut de Ciència de Materials de Barcelona, CSIC, Campus de la UAB, 08193 Bellaterra, Spain*

(Received 11 August 2010; accepted 30 October 2010; published online 23 December 2010)

Epitaxial thin films of biferroic $(\text{Bi}_{1-x}\text{La}_x)_2\text{NiMnO}_6$ have been grown on SrTiO_3 (001) substrates. High resolution electron microscopy, energy-loss spectroscopy and synchrotron radiation have been used to demonstrate that, under appropriate growth conditions, stoichiometric, and fully oxidized thin films with long-range order of Ni^{2+} and Mn^{4+} ions can be obtained, despite the presence of randomly distributed dissimilar cations (Bi, La) at the A-site. This ordering leads to $\text{Ni}^{2+}\text{--O--Mn}^{4+}$ ferromagnetic interactions and its preservation in thin films is key for implementation of these biferroic materials in practical devices. © 2010 American Institute of Physics.

[doi:10.1063/1.3524278]

I. INTRODUCTION

Multiferroic materials, in which coexistence of both ferroelectric and (anti)ferromagnetic order takes place, have received much interest in the last few years.¹ This interest is steered by the promising applications these materials could have in magnetoelectronic devices.² However, multiferroic materials are scarce in nature, especially ferromagnetic multiferroics, since antiferromagnetism, particularly in oxides having a perovskite structure, is in general the predominant magnetic order.

Double-perovskite structures ($\text{A}_2\text{BB}'\text{O}_6$) are very versatile when it comes to designing ferromagnetic ferroelectrics because of the possibility of combining different transition metal ions at the B-site. One of these examples is $\text{Bi}_2\text{NiMnO}_6$ (BNMO), which has recently drawn much attention because of its relatively high ferromagnetic transition temperature (140 K) and its ferroelectric character.³ Its ferromagnetic behavior is due to the 180° -bond-angle superexchange interaction between Ni^{2+} ($t_{2g}^6e_g^2$: half-filled e_g orbitals) and Mn^{4+} ($t_{2g}^3e_g^0$: empty e_g orbitals) through the adjacent oxygen ions. Long-range B-site order is required for a fully ferromagnetic character as $\text{Ni}^{2+}\text{--O--Ni}^{2+}$ and $\text{Mn}^{4+}\text{--O--Mn}^{4+}$ give rise to antiferromagnetic interactions. Ferroelectricity in BNMO, like in BiMnO_3 , is thought to be originated by the off-center symmetry distortion caused by the strong covalent bond of Bi^{3+} and O^{2-} ions and the off-center displacement of the so-called lone-pair electrons of $6s^2$ Bi^{3+} orbitals.⁴ The ferroelectric transition temperature was proposed to be above room temperature, around 485 K, and inferred from the occurrence of a phase transition from noncentrosymmetric

monoclinic $C2$ to centrosymmetric monoclinic $P2_1/n$ together with an anomaly in the dielectric permittivity.³

Partial replacement of Bi^{3+} by La^{3+} cations at the A-site has been proved to facilitate single-phase stabilization in bismuth manganite compounds.⁵ Using this approach we recently showed that single phase $(\text{Bi}_{0.9}\text{La}_{0.1})_2\text{NiMnO}_6$ (BLNMO) thin films can be obtained.⁶ On the other hand, B-site ordered $\text{La}_2\text{NiMnO}_6$ (LNMO) is also a ferromagnetic insulator with a Curie temperature (around 280 K) notably higher than BNMO, but it is centrosymmetric and therefore not ferroelectric.⁷ In bulk, the crystal structure of the solid solution $(\text{Bi}_{1-x}\text{La}_x)_2\text{NiMnO}_6$ was proved to be noncentrosymmetric for $x \leq 0.2$, which would enable this compound to be ferroelectric.⁸ Indeed, ferroelectric switching current has been revealed by the so-called positive-up-negative-down measurements⁹ performed on our BLNMO films, demonstrating, conclusively, the unequivocal ferroelectric character.¹⁰ A solid solution of both materials, $(\text{Bi}_{1-x}\text{La}_x)_2\text{NiMnO}_6$, might be, hence, worth studying not only because of the possibility of modifying (increasing) the Curie temperature, but also because the presence of La might reduce the ferroelectric transition temperature and a potential approaching of the ferroelectric and ferromagnetic transition temperatures may enhance the magnetoelectric coupling.^{11,12}

It remains to be ascertained if the typical nonequilibrium conditions used for thin film growth and/or the presence of randomly distributed dissimilar cations at the A-site (Bi, La) constitute key detrimental factors for the required long-range (B, B') order. In this work, we will show that, under appropriate growth conditions, long-range ordering of Ni^{2+} and Mn^{4+} ions can be obtained and thus the potential detrimental role of La/Bi disorder is denied. Moreover, we will show that

^{a)}Electronic mail: eric.langenberg@ub.edu.

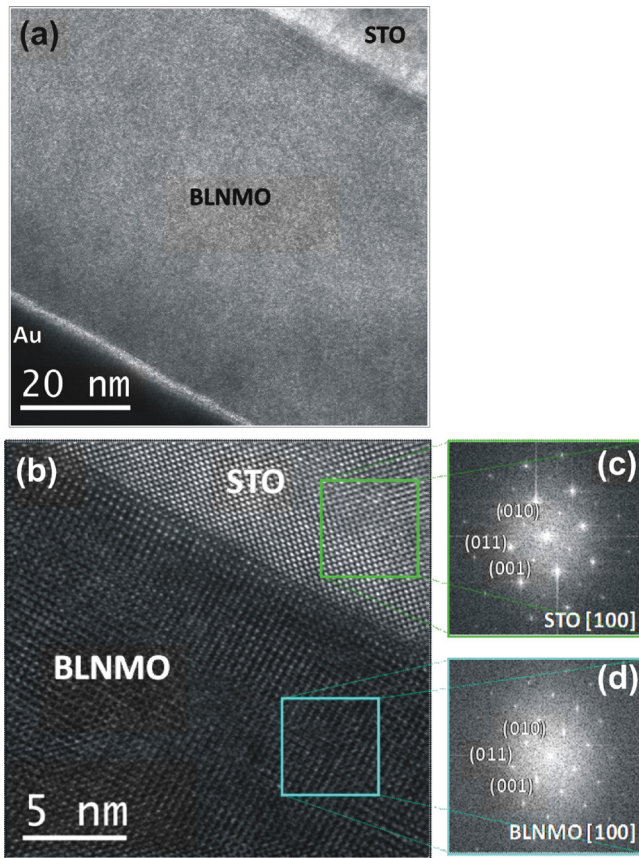


FIG. 1. (Color online) (a) TEM image of [100] cross section; (b) HRTEM image along the [100] zone axis; (c) and (d) are digital power spectrum (FFTs) of the highlighted regions.

the cationic stoichiometry and electronic configuration of the transition metals is that required for ferromagnetic coupling.

II. EXPERIMENTAL

Epitaxial BLNMO thin films were grown by pulsed laser deposition on (001) SrTiO_3 (STO) substrates as reported elsewhere.⁶ Data reported here correspond to a 70 nm thick film. Due to the high volatility of Bi and the poor stability of bismuth manganite compounds,^{5,13–15} single-phase stabilization, without traces of spurious phases, was found to be only possible under a narrow window of deposition conditions.⁶ Synchrotron x-ray diffraction (XRD) and electron diffraction measurements have been performed for the direct observation of the B-site order of the samples. Morphology and structure of the films have been assessed by (scanning) transmission electron microscopy [(S)TEM] and high resolution transmission electron microscopy (HRTEM). Electron energy-loss spectroscopy (EELS) was carried out for compositional and oxidation state analysis. TEM samples were prepared by focused ion beam (FIB). Magnetic measurements have been done using a superconducting quantum interference device magnetometer with in-plane applied magnetic field.

III. RESULTS

TEM images [Fig. 1(a)] of cross sections evidence that BLNMO thin films are very homogeneous and defect-free.

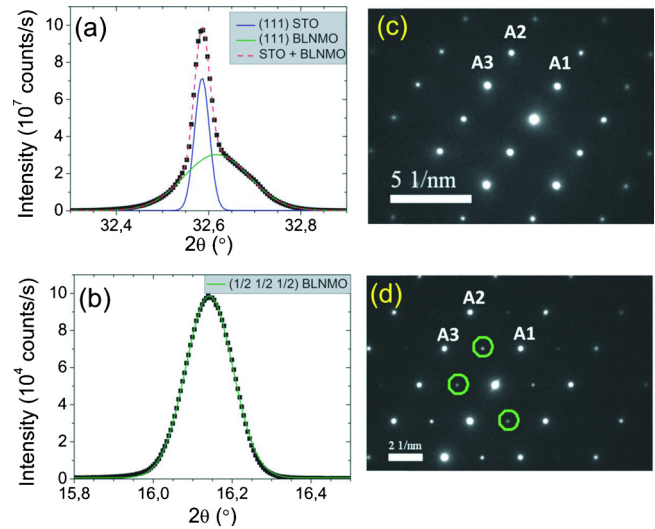


FIG. 2. (Color online) (a) $\theta/2\theta$ synchrotron XRD scan around the fundamental perovskite (111) reflexion of $(\text{Bi}_{0.9}\text{La}_{0.1})_2\text{NiMnO}_6$ and SrTiO_3 . (b) $\theta/2\theta$ synchrotron XRD scan around the $(1/2\ 1/2\ 1/2)$ superstructure reflexion of $(\text{Bi}_{0.9}\text{La}_{0.1})_2\text{NiMnO}_6$. (c) Electron diffraction patterns of the substrate along the $[1\bar{1}0]$ zone axis. A1, A2, A3 spots correspond to the diffraction of (001), (111), and (110) planes, respectively; (d) electron diffraction patterns with contribution of both substrate and BLNMO film. Encircled spots correspond to the superstructure reflexions.

The high crystalline quality of BLNMO films can be appreciated in HRTEM images [Fig. 1(b)]. The BLNMO/STO interface is strikingly sharp. According to the fast Fourier transform (FFT) obtained from substrate and film [Figs. 1(c) and 1(d), respectively], BLNMO films grow coherently on STO substrate, in agreement with XRD data.⁶

Long-range B-site order implies the alternation of Ni-planes and Mn-planes along the $\langle 111 \rangle$ direction. As a consequence of this periodicity, $(1/2\ 1/2\ 1/2)$ superstructure XRD peak should be observed. Its intensity is, however, very low because of the similarity of the atomic scattering factor of Ni^{2+} and Mn^{4+} , so that Synchrotron x-ray radiation was used. Figures 2(a) and 2(b) depict $\theta/2\theta$ synchrotron XRD scan around (111) and $(1/2\ 1/2\ 1/2)$ BLNMO reflexions, respectively. Due to the similar lattice parameters of BLNMO and STO,⁶ Fig. 2(a) shows the contribution of the fundamental perovskite (111) reflexion of both film and substrate ($2\theta_{\text{film}} \approx 32.62^\circ$ and $2\theta_{\text{substrate}} \approx 32.59^\circ$, respectively). In contrast, as superstructure order is absent in STO, the sole contribution observed in Fig. 2(b) should correspond to $(1/2\ 1/2\ 1/2)$ BLNMO reflexion. Indeed, the peak appears around $2\theta \approx 16.14^\circ$, as expected, since, according to the Bragg law, it must fulfill the relation $\sin(\theta_{(1/2\ 1/2\ 1/2)}) = (1/2) \cdot \sin(\theta_{(111)})$, given the fact that the distance between (111) planes and $(1/2\ 1/2\ 1/2)$ planes is $d_{(1/2\ 1/2\ 1/2)} = 2 \cdot d_{(111)}$. Therefore, Fig. 2(b) reveals the long-range B-site order of BLNMO thin films.

Additionally, B-site order was also borne out by electron diffraction. In order to detect the superstructure diffraction peaks, FIB cross sections were prepared along the $[1\bar{1}0]$ zone axis enabling the observation of the reflexions related to the $\{111\}$ planes. In this orientation, selected area electron diffraction patterns from pure substrate regions, Fig. 2(c), show the A1, A2, and A3 spots corresponding to the (001),

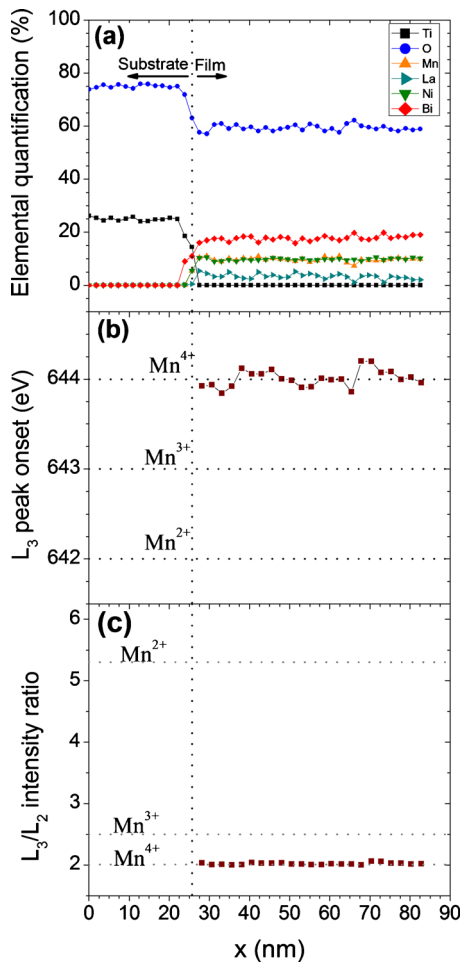


FIG. 3. (Color online) (a) Elemental quantification. The vertical dotted line indicates the interface between STO and BLNMO; (b) Mn L_3 peak onset and (c) Mn L_3/L_2 intensity ratio along the film thickness. Elemental quantification and L_3/L_2 intensity ratio are subjected to a relative error of about 5%. L_3 peak onset is subjected to a ± 0.4 eV error.

(111), and (110) planes, respectively. In diffraction patterns from regions including the film, Fig. 2(d), additional spots (encircled) are found along the $\langle 111 \rangle$ directions which correspond to the $(1/2 \ 1/2 \ 1/2)$ weak diffraction peaks.

Hence, we can conclude that, despite the presence of randomly distributed La and Bi cations at the A-site, long-range B-site order is realized in $(\text{Bi}_{0.9}\text{La}_{0.1})_2\text{NiMnO}_6$ films. Magnetic properties are not solely determined by the B-site order but also by the precise stoichiometry and valence state of the existing species. This is particularly relevant as the highly volatile bismuth¹⁵ may lead to cationic defects that, in turn, may modify the electronic configuration of Ni/Mn ions or the oxygen contents.

EELS compositional profiles obtained in $[100]$ cross section orientation were acquired in perpendicular direction to BLNMO/STO interface. They have been determined from general spectra, in the low-loss (between 40 and 470 eV) and core-loss (between 420 and 930 eV) regions. The concentration of the different species is depicted in Fig. 3(a), in which, accordingly, no ionic interdiffusion across the interface is found. Neither does there seem to be noticeable cationic segregations along the film thickness, as it occurs with La in $(\text{La,Ca})\text{MnO}_3$ thin films grown on STO (001).¹⁶ The film

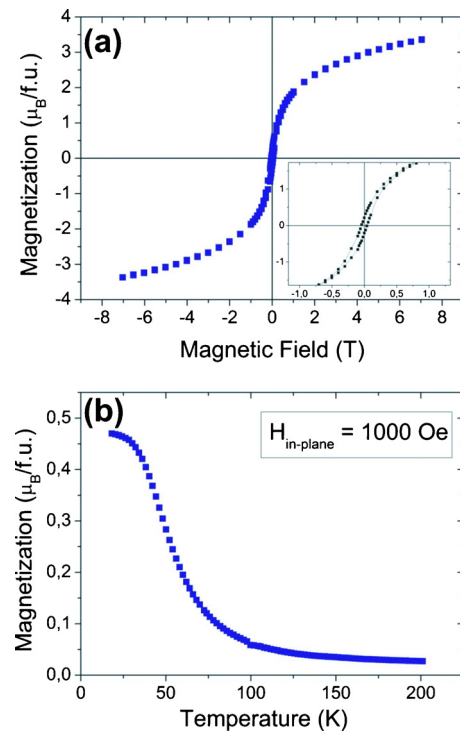


FIG. 4. (Color online) (a) Magnetic field dependence of the magnetization of BLNMO thin film at 10 K. Bottom inset: zoom of the low-field region; (b) temperature dependence of the magnetization under an external in-plane magnetic field of 1000 Oe. Substrate diamagnetic contribution has been subtracted in both figures.

composition is highly stoichiometric and homogeneous. The O and Bi contents normalized by Mn content are around the nominal values: 6 and 1.8, respectively; and the compositional relationship between Ni and Mn is, as expected, 1:1.

EELS spectra in the 400–750 eV energy-loss range was also recorded, where Mn $L_{2,3}$ edges take place. These peaks are known to be related to the formal valence of manganese ions,^{16,17} as Mn L_3 peak position is shifted to higher energies on decreasing the occupancy of d orbitals, whereas L_3/L_2 intensity ratio decreases when the orbital configuration varies from d^5 to d^0 or d^{10} . The expected energy positions of L_3 edges and intensity ratios L_3/L_2 corresponding to the different oxidation states of Mn ions are depicted in dotted lines in Figs. 3(b) and 3(c). The collected data, determined by using a home-made software package MANGANITAS,^{16,18,19} evidences the homogeneity of Mn^{4+} within BLNMO films.

Likewise, the Ni oxidation state has been assessed by Ni L_2 and L_3 edges, which occur at 872 eV and 855 eV, respectively. The determined fine structure of these $L_{2,3}$ edges corresponds to the divalent oxidation state.²⁰

We now turn on to the magnetic properties. Data of previous paragraphs clearly indicates that BLNMO films are B-site ordered, fully stoichiometric and the electronic configuration of Ni^{2+} and Mn^{4+} ions are those required for ferromagnetic coupling. An ideal ferromagnetic ordering of the spins of the B-cations, Ni^{2+} ($t_{2g}^6 e_g^2, S=1$) and Mn^{4+} ($t_{2g}^3, S=3/2$), implies a saturated magnetization $M_S=5 \mu_B/\text{f.u.}$ Magnetization data of Fig. 4(a) shows that the film does not saturate even at the highest field. Notice that the diamagnetic substrate contribution has been subtracted from raw data.

Our films have a magnetization M_S (7 T, 10 K) $\approx 3.5 \mu_B/\text{f.u.}$, in close agreement with data reported for bulk $(\text{Bi}_{0.9}\text{La}_{0.1})_2\text{NiMnO}_6$ samples ($M_S \approx 3.6 \mu_B/\text{f.u.}$), which, we recall, do not saturate, either, even at 7 T and 5 K.⁸ The presence of some antisite defects and antiphase boundaries, common defects in double perovskites structures,²¹ may account for both the hardness to saturation and the accompanying reduced magnetization as found here. The magnetic remanence, as shown in Fig. 4 (bottom panel) is rather low probably due to the small spin-orbit coupling of the magnetic ions.

On the other hand, inspection of the temperature dependent magnetization data [Fig. 4(b)] indicates that the Curie transition occurs at $T_C \approx 100$ K. This value is lower than the bulk one of BNMO (≈ 140 K),³ but, nonetheless, in agreement with the reduced Curie temperature found for BNMO thin films.^{22,23} This reduction in the magnetic transition temperature can be ascribed to the epitaxial stress exerted by the substrate.^{6,22} The rather broad transition temperature could also result from some distribution of superexchange interactions within the sample, likely driven by the distinct length and angles of Ni–O–Mn bonds around A-site occupied either by La or Bi cations.

IV. CONCLUSIONS

In summary, we have shown that under appropriate growth conditions, epitaxial and stoichiometric thin films of BLNMO can be grown on STO (001) substrates. Importantly enough, long-range order of Ni^{2+} and Mn^{4+} ions at B-sites in this double perovskite has been observed. This key finding clearly demonstrates that Ni^{2+} –O– Mn^{4+} bonds and its long-range order are responsible for the ferromagnetic character of BLNMO thin films. We have proved that this critical condition can be achieved in thin film as observed in bulk. In spite of this, the magnetic transition and the saturation magnetization are found to be, as already found in bulk materials, somewhat smaller than that expected and we claimed that this could be related to antiphase boundaries and the Bi/La disorder at A-site. Therefore, our results show that $(\text{Bi}_{1-x}\text{La}_x)_2\text{NiMnO}_6$ films can be successfully implemented in biferroic thin film-based devices.

ACKNOWLEDGMENTS

Financial support by the Ministerio de Ciencia e Innovación of the Spanish Government (Grant No. BES-2006–

12948 and Project Nos. MAT2005-05656-C04, MAT2008-06761-C03, MAT2008-06761-C04, NANOSELECT CSD2007-00041, and IMAGINE CSD2009-00013, and the European Union (Project Nos. MaCoMuFi-FP6-033221, FEDER, and 2009 SGR 00376) is acknowledged. Synchrotron facilities at HASYlab, DESY (Deutsches Elektronen-Synchrotron) in Hamburg (Germany) are acknowledged.

¹R. Ramesh and N. Spaldin, *Nature Mater.* **6**, 21 (2007).

²M. Gajek, M. Bibes, S. Fusil, K. Bouzehouane, J. Fontcuberta, A. Barthélémy, and A. Fert, *Nature Mater.* **6**, 296 (2007).

³M. Azuma, K. Takata, T. Saito, S. Ishiwata, Y. Shimakawa, and M. Takano, *J. Am. Chem. Soc.* **127**, 8889 (2005).

⁴A. Ciucivara, B. Sahu, and L. Kleinman, *Phys. Rev. B* **76**, 064412 (2007).

⁵M. Gajek, M. Bibes, F. Wyczisk, M. Varela, J. Fontcuberta, and A. Barthélémy, *Phys. Rev. B* **75**, 174417 (2007).

⁶E. Langenberg, M. Varela, M. V. García-Cuenca, C. Ferrater, M. C. Polo, I. Fina, L. Fàbrega, F. Sánchez, and J. Fontcuberta, *J. Magn. Magn. Mater.* **321**, 1748 (2009).

⁷N. S. Rogado, J. Li, A. W. Sleight, and M. A. Subramanian, *Adv. Mater.* **17**, 2225 (2005).

⁸Y. Kobayashi, M. Shiozawa, K. Sato, K. Abe, and K. Asai, *J. Phys. Soc. Jpn.* **77**, 084701 (2008).

⁹J. F. Scott, L. Kammerdiner, M. Parris, S. Traynor, V. Ottenbacher, A. Shawabkeh, and W. F. Oliver, *J. Appl. Phys.* **64**, 787 (1988).

¹⁰E. Langenberg, I. Fina, C. J. M. Daumont, J. Ventura, L. E. Coy, M. C. Polo, M. V. García-Cuenca, C. Ferrater, B. Noheda, M. Varela, and J. Fontcuberta, (unpublished).

¹¹T. Kimura, S. Kawamoto, I. Yamada, M. Azuma, M. Takano, and Y. Tokura, *Phys. Rev. B* **67**, 180401(R) (2003).

¹²C.-H. Yang, S.-H. Lee, T. Y. Koo, and Y. H. Jeong, *Phys. Rev. B* **75**, 140104 (2007).

¹³S. Fujino, M. Murakami, S.-H. Lim, L. G. Salamanca-Riba, M. Wuttig, and I. Takeuchi, *J. Appl. Phys.* **101**, 013903 (2007).

¹⁴E. Langenberg, M. Varela, M. V. García-Cuenca, C. Ferrater, F. Sánchez, and J. Fontcuberta, *Mater. Sci. Eng., B* **144**, 138 (2007).

¹⁵N. Dix, R. Muralidharan, B. Warot-Fonrose, M. Varela, F. Sánchez, and J. Fontcuberta, *Chem. Mater.* **21**, 1375 (2009).

¹⁶S. Estradé, J. Arbiol, F. Peiró, I. C. Infante, F. Sánchez, J. Fontcuberta, F. de la Peña, M. Walls, and C. Colliex, *Appl. Phys. Lett.* **93**, 112505 (2008).

¹⁷H. Kurata and C. Colliex, *Phys. Rev. B* **48**, 2102 (1993).

¹⁸S. Estradé, J. Arbiol, F. Peiró, Ll. Abad, V. Laukhin, Ll. Balcells, and B. Martínez, *Appl. Phys. Lett.* **91**, 252503 (2007).

¹⁹S. Estradé, J. M. Rebled, J. Arbiol, F. Peiró, I. C. Infante, G. Herranz, F. Sánchez, J. Fontcuberta, R. Córdoba, B. G. Mendis, and A. L. Beloch, *Appl. Phys. Lett.* **95**, 072507 (2009).

²⁰P. L. Potapov, S. E. Kulkova, D. Schryvers, and J. Verbeeck, *Phys. Rev. B* **64**, 184110 (2001).

²¹J. Navarro, L. L. Balcells, F. Sandiumenge, M. Bibes, A. Roig, B. Martínez, and J. Fontcuberta, *J. Phys.: Condens. Matter* **13**, 8481 (2001).

²²M. Sakai, A. Masuno, D. Kan, M. Hashisaka, K. Takata, M. Azuma, M. Takano, and Y. Shimakawa, *Appl. Phys. Lett.* **90**, 072903 (2007).

²³P. Padhan, P. LeClair, A. Gupta, and G. Srinivasan, *J. Phys.: Condens. Matter* **20**, 355003 (2008).